2015 IEEE International Conference on Robotics and Automation (ICRA)
Washington State Convention Center
Seattle, Washington, May 26-30, 2015

Two steps is enough: no need to plan far ahead for walking balance

Petr Zaytsev†, S. Javad Hasaneini†, and Andy Ruina†

Abstract— **Before designing a controller in detail, we ask this question:** ***for a given robot state, and every possible control action, what is the minimum number of steps needed to get to a given target state (if it is possible to do so)?*** **Our biped model is a 2D inverted pendulum with massless legs. We have two controls: (i) the magnitude of an impulsive push-off just before heel-strike and (ii) the step length (location of the next heel-strike). The maximum impulse and minimum step time are bounded to reflect limited motor strength. We compute the set of initial mid-stance velocities from which the biped can reach a given target mid-stance velocity in n or fewer steps. The result: for most target speeds and initial velocities, and with realistically strong actuators, it is possible to reach the target in two steps, if it is possible to reach it at all. This 'two steps is enough' result expands on Koolen *et al.*'s [1] results for capturability of the linear inverted pendulum and is consistent with some human balance and visual guidance experiments.**

I. Introduction

With faster and faster available computation, a sensible way to control locomotion is with Model-Predictive Control, MPC [2]. MPC uses on-the-fly model-based trajectory optimizations to determine the best controls to reach a desired target from the present given state. The controls based on this model-based prediction are updated as rapidly as possible.

One MPC design freedom is the 'horizon'; how far ahead in time the optimizer plans. Koolen *et al.* [1] hypothesize that at any instant during locomotion, humans are able to come to a stop, if they choose, within three steps. Koolen *et al.* also argue that present 3D bipedal robots can usually, with appropriate controls, stop within two steps. Using stopping as a proxy for general targets, Koolen *et al.* are thus arguing that 2 or 3 steps look-ahead is sufficient for motion planning.

This two-or-three-step claim is consistent with some experiments on human walking balance [3], [4] and visual guidance [5], [6]. Also similar observations have been made for control of hopping robots [7], [8] (see section V for further discussion). Here, we use the inherently more-energy-efficient inverted pendulum model instead of the linear-inverted pendulum used by Pratt's group, because it more closely matches the robots in our lab. We also generalize the standing-still target to the target of walking at a desired, possibly non-zero, speed. The paper supports, by means of these examples, the following claim:

Two-step controllability: *For a given model of a biped and an arbitrary target, if it is possible for the biped to reach the target at all, in most cases it can be done in two steps or fewer.*

†Sibley School of Mechanical and Aerospace Engineering, Cornell University, Ithaca, New York, USA, 14853. {pvz3, hasaneini, ruina}@cornell.edu

Why does it matter? The 'two-step controllability' claim, if valid for complex real robots, suggests that MPC controllers can generally set their planning horizon at two steps. This is a huge computational advantage for high-dimensional systems in which optimization calculations are limited by processor speed, processor size and processor energy use. We plan to use some version of model based control on our coming robots, using simplifications suggested by this paper.

II. Background concepts and definitions

A walking robot has a state which evolves according to the laws of mechanics as influenced by the controlled actuations. A given system state is *controllable*[1] to a specified target if there is some set of controls that lead the system to the target in finite time without intermediate failure. Two example targets are: 1) standing still (as for Pratt's capturability [11]), and 2) moving at a specific forward speed. More general targets in location or state (*e.g.* overall robot configuration or following a path) are possible but are not considered here. Example failures include falling, exceeding motor limits, or exceeding joint-angle bounds.

For a given model, target and failure rules, a given robot state is either controllable or not. The *controllable region*, a subset of the state space, is the set of all controllable states.

We monitor the system's state only at a Poincaré section (*e.g.* mid-stance), considering a step as a map from one crossing through the Poincaré section to the next. We call a given state and set of control actions *viable* or *non-failed*, if none of the model's constraints is violated during the step. Let C_0 be the set of all states on the Poincaré section that fit a goal description; the goal set C_0 is the *target region*[2] (our generalization of Koolen *et al*'s standing still on one foot). We define the n*-step controllable region* C_n for $n \geq 1$ as the set of all states on the Poincaré section from which the biped can, with some feasible controls, reach one of the target states in C_0 in n or fewer viable steps. Equivalently, C_n is the set of all states on the Poincaré section from which the robot can get to C_{n-1} within one viable step. The definition of C_n implies that the sequence $\{C_n\}$ is nested, $C_{n-1} \subset C_n$ for any $n \geq 1$, and we call its limit the ∞*-step controllable region* C_∞. The region C_∞ is the set of all states on the

[1]Our 'controllability' is called *capturability* in [9] and applies to an arbitrary target. However, Pratt's group uses 'capturability' [1] only for the particular target of coming to a complete stop standing on one foot. Our 'controllability' is close to that used in classical Control theory [10].

[2]Although controllable regions can be considered for target states that are either failed or preventing a failure is impossible once at them, we limit ourselves to the target states from which it is possible to continue the motion forever without a failure. From the Viability theory's [9] point of view, we limit our targets to the *Viability Kernel* of our system.

978-1-4799-6923-4/15/$31.00 ©2015 IEEE

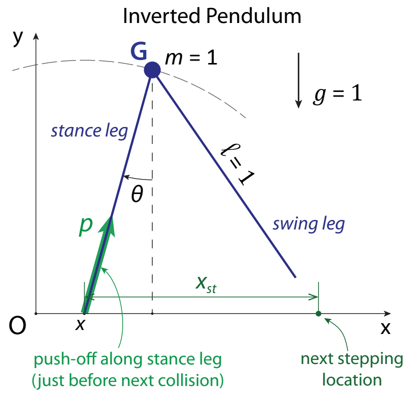

Fig. 1. **Planar Inverted Pendulum (IP) model of walking** has a point mass m at the hip (G) and two rigid inextensible massless legs. There are two control parameters at each step: push-off impulse p just before the foot-ground contact, and step length $x_{\rm st}$ determining the time and location of the contact. The motion of the massless swing leg has no effect on the stance leg dynamics.

Poincaré section from which the biped can either reach the target C_0 in a finite number of steps or at least approach it asymptotically.

If our goal set C_0 is a full stop, our C_n is Koolen *et al.*'s n-step viable-capture basin.

Knowing a state is controllable does not tell you what controls are needed to reach the target, only that they exist. The *extended controllable regions* $\bar{C}_n$ bring the controls into play. The pair (q, u) is the *extended state*, where q is the state of the robot on its Poincaré section, and u the vector of controls for the next step. The *extended n-step controllable region* $\bar{C}_n$ is the set of all extended states (q, u) such that starting from the state q on the Poincaré section and using the controls u during the first step the robot can reach the target C_0 in n or fewer viable steps. Equivalently, $\bar{C}_n$ is all extended states, for which the $(n-1)$-step controllable region C_{n-1} can be reached in one viable step. That is, $\bar{C}_n$ is the extended 1-step controllable region corresponding to the target C_{n-1}. The sequence $\{\bar{C}_n\}$ of the extended regions is nested ($\bar{C}_{n-1} \subset \bar{C}_n$), and we call its limit the *extended ∞-step controllable region* $\bar{C}_\infty$. $\bar{C}_\infty$ is the set of all extended states (q, u) starting from which the target can be reached, at least asymptotically.

We also consider partial extended controllable regions by including only the controls of interest in the control vector u. We indicate this with a superscript. For example, $\bar{C}_n^p$ is the extended n-step controllable region when only control parameter p is included in u and other controls are free to be determined.

III. Biped and Walking Model

We use a standard 2D Inverted Pendulum (IP) model [12], [13] with a point mass m at the hip and two identical massless rigid legs of fixed length ℓ (Fig. 1). Only walking on a flat ground is considered. As a standard assumption in compass gait models [12]-[15], swing-foot scuffing at mid-swing is ignored. At foot-ground contact (heel-strike) an instantaneous and plastic (no bounce) collision happens, and support is instantaneously transferred from the trailing to the leading leg (instantaneous double stance). Just before heel-strike, a push-off impulse p is applied along the stance leg. Due to the push-off and heel-strike impulses, the hip velocity is discontinuous at instantaneous support transfer.

State and control variables. We consider mid-stance ($\theta = 0$) as the Poincaré section (an event surface) of our biped model, making the problem discrete and lower-dimensional. At mid-stance the biped state is characterized by the stance-leg angular rate $\dot{\theta}$; the motion of the massless swing leg is irrelevant. The controller can move the swing leg to any desired orientation, thus determining the step-length $x_{\rm st}$ (the distance between the two feet at heel-strike). The controller also determines the push-off p at support transfer, but between collisions the stance leg motion is not controlled. Our model is thus reduced to one state variable, $\dot{\theta}$ at mid-stance, and two control parameters per each step, the step size $x_{\rm st}$ and the push-off p.

Gait dynamics. We non-dimensionalize all variables using the hip mass m, leg length ℓ, and the gravity constant g: time and force are non-dimensionalized by $\sqrt{\ell/g}$ and mg, respectively. Equivalently, we set $m = \ell = g = 1$ in all equations.

The step-to-step map is calculated in two phases: 1) continuous single stance and 2) discontinuous collisional support transfer. In single stance we use inverted-pendulum equations. At the support transfer (push-off + heel-strike), angular momentum balance about the new stance foot determines the (new) stance leg angular rate, *i.e.* $\dot{\theta}^+$, from the (former) stance leg angular rate just before push-off, *i.e.* $\dot{\theta}^-$:

$$\dot{\theta}^+ = \dot{\theta}^- \cos 2\theta_{\rm sw} - p \sin 2\theta_{\rm sw}. \tag{1}$$

Here, $\theta_{\rm sw} < 0$ is the swing leg angle at heel-strike and can be used as a proxy for step length, given by

$$x_{\rm st} = -2 \sin \theta_{\rm sw}. \tag{2}$$

Walking constraints. A 'viable' step is a non-failed step; it has no flight phase, makes it up to the next mid-stance, and meets other constraints, listed below.

The compression in the stance leg is always non-negative:

$$\text{leg compression} = F_{\rm st} = -\dot{\theta}^2 + \cos\theta \geq 0. \tag{3}$$

Because $F_{\rm st}$ increases as the robot moves from heel-strike to mid-stance and decreases again until push-off, we need only check (3) just before push-off and just after heel-strike:

$$\cos\theta_{\rm sw} - (\dot{\theta}^-)^2 \geq 0, \qquad \cos\theta_{\rm sw} - (\dot{\theta}^+)^2 \geq 0. \tag{4a}$$

Similarly, the heel-strike impulse must be non-negative, so the hip velocity just before heel-strike (just after push-off) must have a downward component along the leading leg. This along with a non-negative push-off constraint is expressed as

$$p \cos 2\theta^- - \dot{\theta}^- \sin 2\theta^- \leq 0, \qquad \text{and} \qquad p \geq 0. \tag{4b}$$

Step map. For the controllability analysis, we would like to map the initial mid-stance state $\dot{\theta}_0$ and two controls, step size $x_{\rm st}$ and push-off p, to the state $\dot{\theta}_1$ at the next mid-stance. For this purpose, we use conservation of energy to find $\dot\theta^-$ from $\dot\theta_0$ and $\dot\theta^+$ from $\dot\theta_1$. This, with velocity map at the collision, equation (1), gives our step (or Poincaré) map:

$$\sqrt{2-2\cos\theta_{\rm sw}+\dot\theta_1^2} = -\,p\sin 2\theta_{\rm sw} + \cos 2\theta_{\rm sw}\sqrt{2-2\cos\theta_{\rm sw}+\dot\theta_0^2}. \tag{5}$$

Similarly, the step map constraints, given by equation set (4), can be expressed in terms of $\dot\theta_0$, $\dot\theta_1$, p, and $\theta_{\rm sw}$:

$$\max\left(\dot\theta_0^2,\, \dot\theta_1^2\right) \le 3\cos\theta_{\rm sw} - 2, \tag{6a}$$

$$p\cos 2\theta_{\rm sw} + \sin 2\theta_{\rm sw}\sqrt{2-2\cos\theta_{\rm sw}+\dot\theta_0^2} \le 0, \tag{6b}$$

$$p \ge 0. \tag{6c}$$

The map (5), the step size equation (2), and the three constraints (6) determine all combinations of the initial and final hip velocities, $\dot\theta_0$ and $\dot\theta_1$, and the controls, p and $x_{\rm st}$, that correspond to a viable step. In other words, these equations define the 1-step controllable region C_1 corresponding to a given target velocity $\dot\theta_1$ (see similar derivation in [17]).

IV. Controllable Regions

Now, we compute the controllable regions C_n, and the extended-controllable regions $\bar{C}_n$. For our model the $\bar{C}_n$ regions are 3D (one state and two control variables). To simplify the visualization, we extend the state space by only one control variable at a time, considering $\bar{C}_n^{x_{\rm st}}$ extended by the step size $x_{\rm st}$, and $\bar{C}_n^p$ extended by the push-off p. Although these are the *partial* extended controllable regions, for simplicity we drop the term 'partial' when referring to them.

1-Step controllability. Our target state is a desired velocity $\dot\theta_t$ of the hip at mid-stance. The region $\bar{C}_1^{x_{\rm st}}$ is all combinations $(\dot\theta_0, x_{\rm st})$ for which there is some feasible push-off p, such that the robot reaches the target velocity $\dot\theta_t$ at the next mid-stance with no failure. More formally, $(\dot\theta_0, x_{\rm st})$ is a point in $\bar{C}_1^{x_{\rm st}}$ if $\dot\theta_0$ and $\theta_{\rm sw} = -\sin^{-1}(x_{\rm st}/2)$ satisfy the Poincaré map equation (5) and the three walking constraints (6) for some value of p and the fixed final velocity $\dot\theta_1 = \dot\theta_t$. With algebraic manipulation of (5) and (6), we found analytical expressions for the boundaries of $\bar{C}_1^{x_{\rm st}}$; on each boundary one of the inequalities (6) becomes an equality (for details, see [18]).

Fig. 2b illustrates $\bar{C}_1^{x_{\rm st}}$ for the example $\dot\theta_t = 0.3$ (*i.e.* mid-stance speed ≈ 0.94 m/s for a robot with 1m legs). For any given initial velocity $\dot\theta_0$, a vertical line segment in the dark region $\bar{C}_1^{x_{\rm st}}$ is the range of step sizes available to the step-size controller such that the robot can, with an appropriate push-off p, reach the target velocity $\dot\theta_t$ within one step.

All initial velocities, for which there is at least one step size in $\bar{C}_1^{x_{\rm st}}$ (*i.e.* the projection of $\bar{C}_1^{x_{\rm st}}$ onto the $\dot\theta_0$-axis), constitute the 1-step controllable region C_1, shown in Fig. 2a. If the robot's velocity at mid-stance is outside of C_1, there is no way for the robot to reach the target velocity in one step (*e.g.* for the target $\dot\theta_t = 0.3$, the largest 1-step controllable velocity is $\dot\theta_0 \approx 0.82$).

The set of push-offs p for which it is possible for the robot to reach the target within one step is shown in the extended 1-step controllable region $\bar{C}_1^p$ illustrated in Fig. 2c . This is all combinations of $(\dot\theta_0, p)$ for which there is some feasible step size $x_{\rm st}$ such that the robot reaches the target $\dot\theta_t$ at the next mid-stance. Again, the projection of $\bar{C}_1^p$ onto the $\dot\theta_0$-axis is the 1-step controllable region C_1 shown in Fig. 2a.

n-Step and ∞-step controllability. The n-step controllable region C_n is all initial velocities $\dot\theta_0$, such that the robot can, with appropriate controls, reach the target in n or fewer steps. The corresponding appropriate controls are given by n-step extended controllable regions $\bar{C}_n^{x_{\rm st}}$ (and, respectively, $\bar{C}_n^p$), which are all combinations of velocities $\dot\theta_0$ and step sizes $x_{\rm st}$ (push-offs p) for the *next* step, with which the robot can reach the target within n steps.

Numerical procedure. We compute the regions $\bar{C}_n^{x_{\rm st}}$ and $\bar{C}_n^p$ iteratively: $\bar{C}_n^{x_{\rm st}}$ (or $\bar{C}_n^p$) is the extended 1-step controllable region for the step-size control $x_{\rm st}$ (push-off control p) when the target set is the $(n-1)$-step controllable region C_{n-1}. We discretize C_{n-1} into N grid points and calculate the extended 1-step controllable region corresponding to each grid point. The union of these 1-step regions is the extended n-step controllable region for the ultimate target $C_0 = \dot\theta_t$. Thus, we first calculate $\bar{C}_1^{x_{\rm st}}$, $\bar{C}_1^p$, and C_1 for the ultimate target $\dot\theta_t$, as explained above. Then, for each $n > 1$ we sequentially compute $\bar{C}_n^{x_{\rm st}}$, $\bar{C}_n^p$, and C_n based on the knowledge of C_{n-1}.

Figs. 2b and 2c show, respectively, the regions $\bar{C}_n^{x_{\rm st}}$ and $\bar{C}_n^p$ for $\dot\theta_t = 0.3$. The projections of both $\bar{C}_n^{x_{\rm st}}$ and $\bar{C}_n^p$ onto the $\dot\theta_0$-axis are the n-step controllable regions C_n, shown in Fig. 2a. The regions C_n for the 2D IP model were also derived by Wolfslag [17]. Note the nested structure of the presented regions: $C_n \subset C_{n+1}$ for $n \ge 0$, and $\bar{C}_n^{x_{\rm st}} \subset \bar{C}_{n+1}^{x_{\rm st}}$, $\bar{C}_n^p \subset \bar{C}_{n+1}^p$ for $n \ge 1$.

As n increases, the regions $\bar{C}_n^{x_{\rm st}}$ in Fig. 2b approach the extended ∞-step controllable region $\bar{C}_\infty^{x_{\rm st}}$. Similarly, the regions $\bar{C}_n^p$ in Fig. 2c approach the extended ∞-step controllable region $\bar{C}_\infty^p$. As for the n-step regions, projection of both $\bar{C}_\infty^{x_{\rm st}}$ and $\bar{C}_\infty^p$ onto the velocity axis is the ∞-step controllable region C_∞, shown in Fig. 2a. C_∞ is the limit of the regions C_n as n increases. Computations using a range of target velocities $0 \le \dot\theta_t \le 1$ show that the ∞-step regions C_∞, $\bar{C}_\infty^{x_{\rm st}}$, and $\bar{C}_\infty^p$ are independent of the target; if you are in a state from which you can take viable steps to reach one target other than your current state[3], you could eventually reach any target.

Our central claim shows in Fig. 2: the two-step controllable region C_2 is most ($\sim 95\%$) of the ∞-step controllable region C_∞. Similarly, the extended regions $\bar{C}_2^{x_{\rm st}}$ and $\bar{C}_2^p$ are close to $\bar{C}_\infty^{x_{\rm st}}$ and $\bar{C}_\infty^p$, respectively. This is the 'Two-step controllability' claim: if it is possible to reach a given target at all, in most cases it is possible to reach it within two steps. We generalize the result for cases with actuation limits below.

[3]Our model has no ankle torque, so when standing still on one leg it cannot start moving to reach any target other than its current state.

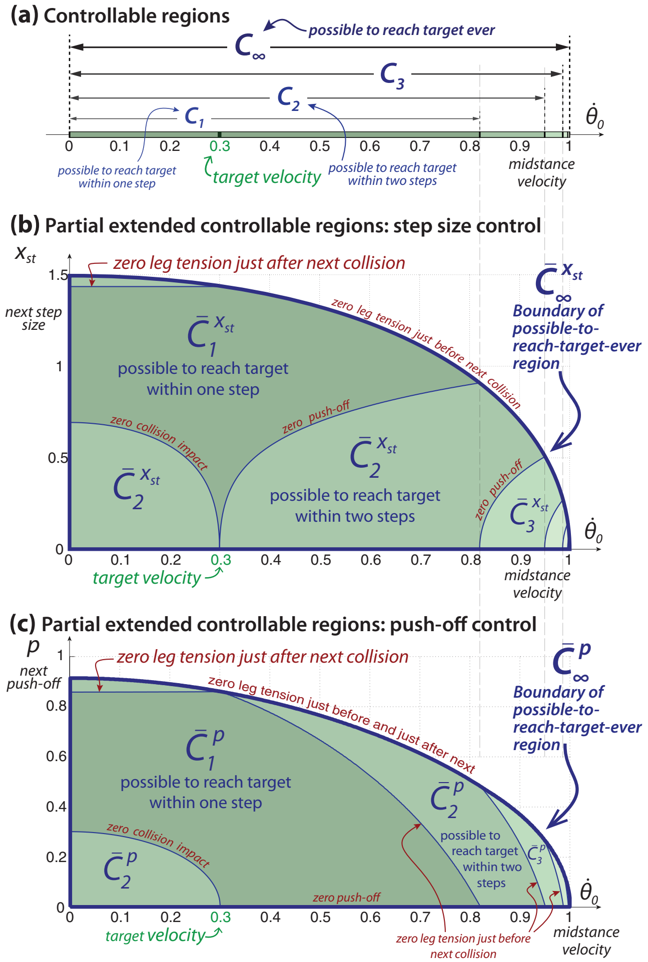

Fig. 2. n**-step controllable regions.** Here $\dot{\theta}_t = 0.3$. Note: C_2 is almost all of C_∞ in all three plots. **(a)** The n-step controllable regions. C_n are the set of initial velocities $\dot{\theta}_0$, for which the robot can reach the target velocity $\dot{\theta}_t$ in n or fewer steps. **(b), (c)** are partial extended regions, supplement the state with the step-size or push off control, respectively. For each $\dot{\theta}_0$, the extended n-step controllable regions $\bar{C}_n^{x_{\rm st}}$ and $\bar{C}_n^{p}$ show, respectively, all step sizes $x_{\rm st}$ and push-offs p of the first step, for which it is possible to reach the target in n or fewer steps. The regions C_n, $\bar{C}_n^{x_{\rm st}}$, and $\bar{C}_n^{p}$ form sequences of nested regions, which approach the ∞-step regions C_∞, $\bar{C}_\infty^{x_{\rm st}}$, and $\bar{C}_\infty^{p}$ (shown by their boundary) correspondingly. Each C_n of figure (a) is the projection of both $\bar{C}_n^{x_{\rm st}}$ and $\bar{C}_n^{p}$ of figures (b) and (c) onto the $\dot{\theta}_0$-axis.

Actuator constraints. In Fig. 2 we allowed arbitrary controls. Now we add constraints, representing limits on push-off and leg-swing motors, and see if the 2-step controllability is maintained. First, we limit the maximum available push-off impulse p:

$$0 \leq p \leq p_{\max}. \tag{7a}$$

Next, we assume that a specified minimum time is needed to swing the leg by imposing a fixed lower bound on the *step time* $t_{\rm st}$, the time from the mid-stance to heel-strike:

$$t_{\rm st} \geq t_{\rm st,min} > 0 \tag{7b}$$

In steady walking the step time $t_{\rm st}$ is about half of the step period.

Following crude estimates on the bounds of our robots, for the example here we use the bounds $p_{\max} = 0.25$ and

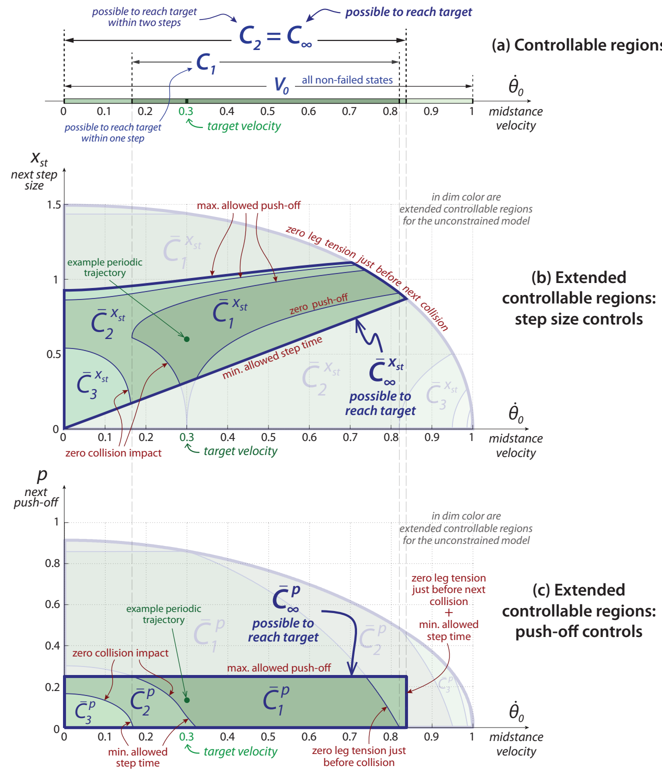

Fig. 3. n**-step controllability of the 2D IP model with limited actuation.** This figure is analogous to Fig. 2, but assumes limited actuation: the maximum allowed push-off is ($p \leq p_{\max}$) and the minimum allowed step time is ($t_{\rm st} \geq t_{\rm st,min}$. We use $p_{\max} = 0.25$, $t_{\rm st,min} = 0.5$. For our constrained model, $C_2 = C_\infty$, $\bar{C}_3^{x_{\rm st}} = \bar{C}_\infty^{x_{\rm st}}$, and $\bar{C}_3^{p} = \bar{C}_\infty^{p}$. The controllable regions for the *un*constrained model (see Fig. 2) are shown dimly in the background.

$t_{\rm st,min} = 0.5$. For comparison, the estimated maximum push-off for the Cornell Ranger robot [19] is ≈ 0.3 and the estimated minimum step-time is 0.4 for Ranger and 0.26 (~ 0.09 s) for humans [20].

We compute the extended controllable regions $\bar{C}_n^{x_{\rm st}}$ and $\bar{C}_n^{p}$ for this constrained model using the same iterative algorithm as for the *un*constrained model (see Fig. 3).

For this example $\bar{C}_n^{x_{\rm st}} = \bar{C}_3^{x_{\rm st}}$ for all $n \geq 3$. Thus, $\bar{C}_3^{x_{\rm st}}$ is equal to the extended ∞-step controllable region $\bar{C}_\infty^{x_{\rm st}}$ (similarly for $\bar{C}_3^{p}$ and $\bar{C}_\infty^{p}$):

$$\bar{C}_\infty^{x_{\rm st}} = \bar{C}_3^{x_{\rm st}}, \qquad \bar{C}_\infty^{p} = \bar{C}_3^{p}. \tag{8}$$

Note, in Fig. 3a the ∞-step controllable region C_∞ is exactly the same as C_2:

$$C_\infty = C_2. \tag{9}$$

That is, if it is possible to reach the target at all, the robot can *always* reach the target in two or fewer steps.

Unsurprisingly, the actuation limits (7) do reduce the size of the extended controllable regions (the regions for the unconstrained model are shown with light shading in Fig. 3). That is, there is a smaller choice of control strategies that bring the robot to the target. However, for this example, these constraints have a smaller effect on the controllability of the robot, *i.e.* on the ∞-step controllable region C_∞. Only in extreme situations (large velocities $\dot{\theta}_0 > 0.84$) the robot is unable to reach the target due to the insufficient actuation.

As suggested by Art Kuo (personal communication), there are actuator limits which violate the observations above. For example, if the robot is allowed fast steps but is highly limited in step size, the C_2 region is no longer a large fraction of C_∞ (for many initial states it takes many steps to reach the target). And if the step time is heavily restricted, the resulting C_∞ is substantially smaller than C_∞ calculated for the unconstrained case. However, these are extreme cases, and under normal circumstances and with practical actuation limits two steps is all needed.

V. If you can't balance in two steps, you can't balance

When a robot deviates from its preferred trajectory, due to an external disturbance, sensor noise, avoiding an obstacle, or because it chooses to change speed, it may take several steps to reach it's target speed. Or, for large disturbances, it may fall. Our goal when designing controllers is to avoid these falls. In picking control strategies, how far ahead do we need to look? The 'Two-step controllability' claim here suggests that in most cases one does not better avoid disaster by looking more than 2 steps ahead. That is, two-step controllability is almost equivalent to ∞-step controllability. This shows in our previous plots by the various C_2 regions being a substantial fraction of the C_∞ regions; for most initial conditions, a target speed can be reached in two steps if it can be reached at all.

In addition to our simple IP model (Fig. 1), there is other support for the 'Two-step controllability' claim: 1) other models; 2) examples of finite-horizon robot control; and 3) some human-subject data. These are discussed below.

Other simple models. Another simple model of walking is the Linear Inverted Pendulum, LIP [21]. The LIP model has a point-mass at the hip and two massless telescopic legs. The leg forces are constrained to keep the hip at a constant height. We have investigated the LIP model in some detail and found similar results as for the IP model here [18]. This slightly generalizes the previous calculations of [1].

Carver *et al.* [7] studied two-step controllability of the Spring-Loaded Inverted Pendulum (SLIP) model, a simple model of hopping and running [22], [23]. The SLIP model has a point-mass body and a massless spring (the leg) attached to it. The controls of the model for each step are the position of the spring-like leg at touch-down (transition from stance to flight) and two spring coefficients (effectively like our push-off parameter) for the stance phase (one for the leg compression, the other for the leg decompression). For a fixed target state (horizontal position, height, and velocity of the point-mass at the flight apex) Carver *et al.* found the set of position perturbations that can be corrected in at most two steps. These perturbations form a large (on the scale of the reference step-size) area surrounding the target location and thus, presumably, most practically-relevant disturbances can be corrected within two steps.

Two-step controls in the robotics community. Two-step control strategies have been used to generate walking controllers [8], [24]. For example, in the animation world, Van de Panne [8] generates the optimal (supposedly most physically realistic) motion of a character for a sequence of desired footstep locations provided *a priori*. Van de Panne finds a two-step horizon control to be sufficient to produce a realistic animation.

Other groups have discovered that planning two or three steps ahead gives sufficient stability for their models [7], [25], [26]. For example, Nishiwaki *et al.* [26] studied the problem of online generation of walking trajectories (of the robot's links) based on a given trajectory of the center of pressure on the ground (ZMP path). Each trajectory is generated as a solution of a Boundary-Value Problem (BVP) and plans two, three, or more steps ahead, trying to satisfy several constraints (such as initial and final conditions, and following of the given ZMP path). Nishiwaki *et al.* found that planning more than three steps ahead negligibly improves the generated trajectories (their smoothness and errors in meeting the constraints).

Evidence from humans. Two types of studies on human subjects provide evidence in support of the 'Two-step controllability' claim. The first investigates recovery strategies of humans after various disturbances during walking or standing. The second aim to understand how humans plan ahead during locomotion, e.g. where they look preparing for the next step.

Hof *et al*. [3] study balance responses of young adults to sideway pushes (3 to 12 $\mathrm{kg\,m\,s^{-1}}$ in magnitude) at different phases of walking. The participants were always able to return to their preferred gait in at most two steps after a push. When it was possible (based on the reaction time of the person, the instant of the push, *etc.*) to move the swing leg to a desired stepping location, balance was regained after the first step. Likewise, Tang *et al*. [4] report that humans can restore balance within two steps after slipping. The slipping was simulated in the experiment by jerking a plate under the colliding leg at the instant of collision; the plate perturbation was $10\,\mathrm{cm}$ in either forward or backward direction at the speed $40\,\mathrm{cm/s}$. Schillings *et al*. [27] research recovery strategies of humans after stumbling over an obstacle. Healthy subjects were walking at a comfortable speed, when a $4.5\,\mathrm{cm}$ tall obstacle was released on the treadmill at different phases of the step cycle. The authors report that the normal gait was usually restored in two steps.

Other research that we use in support of our 'Two-step controllability' claim, studies motion planning in humans. In a series of experiments by Patla *et al*. [5], [28] and Hollands *et al*. [29] human participants were asked to follow a specified path on the floor, while their gaze behavior was monitored. One of the objectives was to understand where and when humans focus their eyes when planning the motion ahead. They found that in some tasks (change of the step length or width, obstacle avoidance [5], raised stepping stones [29]) the participants were looking at the location they were about to step next (*i.e.* one step ahead) most of the time. In other tasks (change of the walking direction [5], stepping stones on flat ground [28]) the subjects, on average, were looking two steps ahead, when they were focusing their eyes on specific areas on the ground.

An interesting two-step result comes from Matthis and Fajen [6], who study performance of humans in the obstacle avoidance task with limited visual information. Human subjects were asked to walk across a room filled with obstacles displayed on the floor by a projector. The obstacles were visible only within one, two, or more step-lengths around the participant. The participants' performance (frequency of collisions) significantly improved when the visibility radius was increased from one to two step lengths. On the other hand, visibility of more than two step lengths ahead weakly affected the performance.

VI. Conclusion

We used a simple bipedal model to study the controllability, the ability to reach a target speed without falling, of bipedal walking. The model has two control parameters for each step: the step size and the amount of push-off impulse. We computed all possible states at mid-stance from which the model can, with appropriate controls, reach a given target speed within n steps. We showed that, generally, if the model is able to reach the target at all, it can do so in two steps or less. This result remains unchanged even if the controls are limited within some practical bounds. We also provided evidence from practical robot control and multiple human walking experiments showing that this capability is also valid for more complicated models and appears to be used by humans.

The above considerations lead us to the following proposition: *two steps is almost everything*. That is, anything a model is capable of doing at all, most likely it can do it in only two steps. Practically, this suggests that in a controller design, there is no need to plan the motion of the robot, at least for balance purposes, more than two steps ahead.

Because, for robots with human-like proportions, no matter the complexity of the upper-body motions, almost all control authority is in the step position and push-off, we believe the results extend to walking of people and of all humanoid robots in almost all situations.

References

[1] T. Koolen, T. De Boer, J. Rebula, A. Goswami, and J. Pratt, "Capturability-based analysis and control of legged locomotion, part 1: Theory and application to three simple gait models," *Int. J. Robot. Res.*, vol. 31, no. 9, pp. 1094–1113, 2012.

[2] C. E. Garcia, D. M. Prett, and M. Morari, "Model predictive control: theory and practicea survey," *Automatica*, vol. 25, no. 3, pp. 335–348, 1989.

[3] A. L. Hof, S. M. Vermerris, and W. A. Gjaltema, "Balance responses to lateral perturbations in human treadmill walking," *J. Exp. Biol.*, vol. 213, no. 15, pp. 2655–2664, 2010.

[4] P.-F. Tang, M. H. Woollacott, and R. K. Chong, "Control of reactive balance adjustments in perturbed human walking: roles of proximal and distal postural muscle activity," *Experim. Brain Res.*, vol. 119, no. 2, pp. 141–152, 1998.

[5] A. Patla and J. Vickers, "Where and when do we look as we approach and step over an obstacle in the travel path?" *Neuroreport*, vol. 8, no. 17, pp. 3661–3665, 1997.

[6] J. S. Matthis and B. R. Fajen, "Visual control of foot placement when walking over complex terrain," *J. Experim. Psychol. Human Percep. Perform.*, vol. 40, no. 1, pp. 105–115, 2013.

[7] S. G. Carver, N. J. Cowan, and J. M. Guckenheimer, "Lateral stability of the spring-mass hopper suggests a two-step control strategy for running," *Chaos: An Interdis. J. Nonlin. Sci.*, vol. 19, no. 2, pp. 026 106–1–026 106–14, 2009.

[8] M. van de Panne, "From footprints to animation," in *Comp. Graph. Forum*, vol. 16, no. 4, 1997, pp. 211–223.

[9] J. P. Aubin, A. M. Bayen, and P. Saint-Pierre, *Viability theory: new directions*. Springer, 2011.

[10] T. Kailath, *Linear systems*. Prentice-Hall Englewood Cliffs, NJ, 1980.

[11] J. Pratt and R. Tedrake, "Velocity-based stability margins for fast bipedal walking," *Fast Motions in Biomechanics and Robotics*, pp. 299–324, 2006.

[12] A. Kuo, "Energetics of actively powered locomotion using the simplest walking model," *J. biomech. eng.*, vol. 124, p. 113, 2002.

[13] A. Ruina, J. E. A. Bertram, and M. Srinivasan, "A collisional model of the energetic cost of support work qualitatively explains leg sequencing in walking and galloping, pseudo-elastic leg behavior in running and the walk-to-run transition," *J. Theor. Biol.*, vol. 237, no. 2, pp. 170–192, 2005.

[14] S. J. Hasaneini, C. J. B. Macnab, J. E. A. Bertram, and H. Leung, "Swing-leg retraction efficiency in bipedal walking," in *Intell. Robot. and Sys. (IROS 2014), 2014 IEEE/RSJ Int. Conf.* IEEE, 2014, pp. 2515–2522.

[15] M. Srinivasan and A. Ruina, "Computer optimization of a minimal biped model discovers walking and running," *Nature*, vol. 439, no. 7072, pp. 72–75, 2005.

[16] J. E. A. Bertram and S. J. Hasaneini, "Neglected losses and key costs: tracking the energetics of walking and running," *J. Exp. Biol.*, vol. 216, no. 6, pp. 933–938, Mar. 2013.

[17] W. Wolfslag, "Basin of attraction of controlled simplest walker," 2012, (unpublished).

[18] P. Zaytsev, "Using controllability of simple models to generate maximally robust walking-robot controllers," Ph.D. dissertation, Cornell University, 2015.

[19] P. Bhounsule, "A controller design framework for bipedal robots," Ph.D. dissertation, Cornell University, 2012.

[20] D. G. Thelen, L. A. Wojcik, A. B. Schultz, J. A. Ashton-Miller, and N. B. Alexander, "Age differences in using a rapid step to regain balance during a forward fall," *J. Gerontol. A - Biol. Sci. Med. Sci.*, vol. 52, no. 1, pp. M8–M13, 1997.

[21] S. Kajita and K. Tani, "Study of dynamic biped locomotion on rugged terrain-derivation and application of the linear inverted pendulum mode," in *Robot. Autom., 1991. Proc., 1991 IEEE Int. Conf.*, 1991, pp. 1405–1411.

[22] M. H. Raibert, *Legged robots that balance*. MIT press Cambridge, MA, 1986, vol. 3.

[23] R. Blickhan, "The spring-mass model for running and hopping," *J. biomech.*, vol. 22, no. 11, pp. 1217–1227, 1989.

[24] H.-o. Lim, Y. Kaneshima, and A. Takanishi, "Online walking pattern generation for biped humanoid robot with trunk," in *Robot. Autom., 2002. Proc. ICRA'02. IEEE Int. Conf.*, vol. 3, 2002, pp. 3111–3116.

[25] T. Buschmann, S. Lohmeier, M. Bachmayer, H. Ulbrich, and F. Pfeiffer, "A collocation method for real-time walking pattern generation," in *Human. Robots, 2007 7th IEEE-RAS Int. Conf.*, 2007, pp. 1–6.

[26] K. Nishiwaki, S. Kagami, Y. Kuniyoshi, M. Inaba, and H. Inoue, "Online generation of humanoid walking motion based on a fast generation method of motion pattern that follows desired zmp," in *Intell. Robot. Sys. (IROS), 2002. IEEE/RSJ Int. Conf.*, vol. 3, 2002, pp. 2684–2689.

[27] A. Schillings, B. Van Wezel, T. Mulder, and J. Duysens, "Muscular responses and movement strategies during stumbling over obstacles," *J. Neurophysiol.*, vol. 83, no. 4, pp. 2093–2102, 2000.

[28] A. E. Patla and J. N. Vickers, "How far ahead do we look when required to step on specific locations in the travel path during locomotion?" *Experim. Brain Res.*, vol. 148, no. 1, pp. 133–138, 2003.

[29] M. Hollands, D. Marple-Horvat, S. Henkes, and A. Rowan, "Human eye movements during visually guided stepping," *J. motor behav.*, vol. 27, no. 2, pp. 155–163, 1995.